Published in final edited form as:
J Periodontol. 2011 December ; 82(12): . doi:10.1902/jop.2011.110103.

Modulation of phosphate/pyrophosphate metabolism to regenerate the periodontium. A novel in vivo approach

Thaisângela L. Rodrigues, DDS, MS[*], **Kanako J. Nagatomo, DDS**[†], **Brian L. Foster, MS**[†,‡], **Francisco H. Nociti Jr., DDS, MS, PhD**[*,†], and **Martha J. Somerman, DDS, PhD**[†,‡]

[*]Department of Prosthodontics and Periodontics, Division of Periodontics, School of Dentistry, Campinas State University, Piracicaba, São Paulo, Brazil

[†]Department of Periodontics, University of Washington, School of Dentistry, Seattle, WA, USA

[‡]Department of Oral Biology, University of Washington, School of Dentistry, Seattle, WA, USA

Abstract

Background—The developing periodontium is sensitive to local levels of phosphate (P_i) and pyrophosphate (PP_i), as demonstrated by cementum phenotypes resulting from loss of function of protein regulators of P_i/PP_i homeostasis. The progressive ankylosis protein (ANK) regulates transport of PP_i, and *Ank* knock-out (KO) mice feature rapidly forming and thick cementum. We hypothesized that, besides affecting cementum formation, decreased extracellular PP_i levels in *Ank* KO mice would also impact cementum regeneration.

Methods—Periodontal fenestration defects (2mm/1mm/0.5mm) were created on the buccal aspects of mandibular molars in *Ank* KO and wild-type (WT) mice. Mandibles were harvested at 15 and 30 days post-surgery for histology, histomorphometry, evaluation of in vivo fluorochrome labeling, and immunohistochemistry(IHC) for proteins including bone sialoprotein (BSP), osteopontin (OPN), dentin matrix protein 1 (DMP1), and ectonucleotide pyrophosphatase/phosphodiesterase 1 (NPP1).

Results—A greater amount of new cementum was observed for *Ank* KO mice at 15 and 30 days post-surgery ($p<0.05$), that was confirmed by fluorochrome labeling showing a higher new cementum appositional activity in the defect areas in *Ank* KO vs. controls. At days 15 and 30 during healing, regenerating cementum and associated cells in *Ank* KO recapitulated expression patterns mapped during development, including limited BSP and positive OPN and DMP1 in the cementum matrix, as well as elevated NPP1 in cementoblasts.

Conclusions—Within the limits of the study, these findings suggest that reduced local levels of PP_i can promote increased cementum regeneration. Therefore, local modulation of P_i/PP_i may be a potential therapeutic approach for achieving improved cementum regeneration.

Keywords

cementum; periodontal regeneration; ankylosis protein; mouse; pyrophosphates; inorganic phosphates

Corresponding Author: Dr. Martha J. Somerman, Department of Periodontics, University of Washington, School of Dentistry, Seattle, WA, 98195-7444. somerman@u.washington.edu.

Conflict of interest: The authors declare no conflicts of interest in these studies.

INTRODUCTION

Predictable regeneration of periodontal tissues following periodontal disease is a major, but currently unrealized, goal of periodontal therapy.[1] In pursuit of treatments that can reverse periodontal destruction, including regeneration of new bone, new cementum, and supportive PDL, attempts have been made to understand cellular and molecular mechanisms and factors regulating formation of these tissues during development and regeneration.[2–4] Toward this goal, we have focused on understanding of the role of phosphate and pyrophosphate in regulation of periodontal tissues, aiming to apply this knowledge towards therapies promoting oral tissue regeneration.

The majority of inorganic phosphate (P_i) in the body exists in the mineralized matrix of bones and teeth as hydroxyapatite (HAP). Maintenance of P_i homeostasis is essential for normal development, maintenance, and repair of teeth and skeletal tissues.[5] Conversely, inorganic pyrophosphate (PP_i) is a potent inhibitor of HAP crystal growth.[6, 7] While P_i balance is governed systemically by the bone-intestine-kidney axis,[5, 8] local PP_i in tissues is primarily controlled by a group of cellular factors. The progressive ankylosis gene (*ANKH* in humans; *Ank* in mouse) encodes a transmembrane protein regulating transport of intracellular PP_i to the extracellular space.[9–11] Ectonucleotide pyrophosphatase phosphodiesterase 1 (NPP1) is a membrane-bound ectoenzyme that can generate PP_i from extracellular nucleoside triphosphates.[12] Tissue-nonspecific alkaline phosphatase (TNAP) is an ectoenzyme that can hydrolyze PP_i, and is present in high levels in the periodontium as well as mineralized tissues of the bones and teeth.[13–15] These three key regulators work in concert to control local levels of PP_i.

The developing periodontium is especially sensitive to the balance of P_i/PP_i, as demonstrated by cementum phenotypes resulting from loss of function of protein regulators of P_i/PP_i homeostasis.[5, 16–20] Previously, we identified the intriguing tooth phenotype in *Ank* mutant and KO mice, characterized by a marked increase in cervical cementum formation.[16, 20] Mice lacking ANK function feature decreased extracellular PP_i, promoting increased apposition of acellular extrinsic fiber cementum (AEFC). Despite rapid cementogenesis, mechanical properties of cementum were not compromised.[18] Histological and immunohistochemical evidence supported PP_i as a critical molecular regulator of both cementum apposition and composition.

Based on these findings, we hypothesized that modulation of local PP_i levels might be a strategy to encourage cementum regeneration. To that end, we employed the *Ank* KO mouse, with deficient extracellular PP_i and increased cementogenesis, in a proof-of-principle study to analyze tissue repair and regeneration in a periodontal fenestration model.

MATERIALS AND METHODS

Animals

Preparation and genotyping of *Ank* KO mice were described previously.[20, 21] Heterozygote breeding pairs were employed to prepare homozygote *Ank* KO mice and age-matched wild type (WT) controls. Mice were sacrificed by cervical dislocation, in accordance with American Veterinary Medical Association panel on euthanasia, and all procedures were approved by the Institutional Animal Care and Use Committee, University of Washington (Seattle, WA, USA). Sample size was calculated using previous studies for a power of 0.8 and an alpha of 0.05.

Experimental design and surgical defects

Surgeries were performed on mice at the age of 5 weeks. General anesthesia was delivered by intraperitoneal administration of 130 mg/kg ketamine with 8.8 mg/kg xylasine. A rodent periodontal fenestration defect model was utilized, modified from the method described by King et al.[22] Ten *Ank* KO mice and ten WT control mice were used, with tissues harvested at predetermined time points following surgery: 15 days (n=5 WT and KO), and 30 days (n=5 WT and KO). Periodontal fenestration defects (approximately 2 mm in width, 1 mm in length, and 0.5mm in depth) were created bilaterally at the buccal aspect of the distal root of first and mesial root of second mandibular molars using an operating microscope at 10–40x magnification (Figure 1). Briefly, the superficial bone was removed using a round dental bur (diameter 2 mm), at high speed under saline irrigation. The distal root of first and mesial root of second mandibular molars were denuded of their periodontal ligament, cementum and superficial dentin using a chisel, avoiding excessive damage to the root, which could compromise endodontic tissue and healing response. Tissues were sutured and Buprenorphine (0.05 mg/kg) was given twice daily for 3 days for pain control following surgery.

Histology

Histological processing was performed as previously described.[20] Briefly, mandibles were removed and sagittally hemisected, with one half prepared for histology and the other used for evaluation of fluorochrome labeling (described below). To prepare samples for use in histology and immunohistochemistry, tissues were fixed in Bouin's solution[§] 24 hrs, thoroughly rinsed with 70% ethanol, and demineralized in AFS solution (10% glacial acetic acid and 1.5% formaldehyde in normal saline solution). Tissues were processed according to standard histological procedures and embedded in paraffin. Serial sections (6 μm) were transversally obtained in an apico-coronal direction of the defect and mounted on charged glass slides. Standard hematoxylin and eosin (H&E) staining was used for morphological examination. High resolution digital images were captured using a light microscope[‖] with a camera[¶] and software[#] attached.

Histomorphometric analyses

The coronal and apical margins of the defect were identified and 5 sections per specimen representing the middle portion of the defect (≈12μm apart) were selected, and the percentage of defect filling (DF) (%), proportion of mineralized tissue (BD) (%), extension of new cementum (ENC) (μm), proportion of cementum-denuded root coverage by new cementum (PRC) (%) and thickness of new cementum (TNC) (μm) were histomorphometrically assessed using an image analysis system.[**] Measurements from the five sections were averaged for a total of 5 mice each for WT and KO, from 15 and 30 days after surgery. Histomorphometric approaches are summarized in Figure 1. DF and BD were obtained by the point-counting technique.[23] A square grid was overlaid on the defect area and the percentage of defect filling (DF) and mineralized tissue (BD) determined over the total area of the defect. A mean percentage value was calculated for each animal for statistical analysis. Extension of new cementum (ENC) and thickness of new cementum (TNC) measurements were obtained by linear measurements, whereas the proportion of cementum-denuded root coverage by new cementum (PRC) was obtained by determination of length of new cementum vs. total extent of the instrumented root. TNC measurements

[§]Electron Microscopy Sciences, Fort Washington, PA, USA
[‖]Nikon Eclipse E400, Nikon Instruments Inc, Melville, NY, USA
[¶]SPOT CCD camera, Diagnostic Instruments, Sterling Heights, MI, USA
[#]Metavue, Molecular Devices, Sunnyvale, CA, USA
[**]Image-Pro Plus 4.5; Media Cybernetics Inc., Silver Spring, MD, USA

were made at fixed distances of 50 μm from mesial and distal edges of pre-existing cementum, and on the central portion of the instrumented root. Histomorphometric parameters were determined by a blinded and calibrated examiner (Intra Class Correlation = 0.92).

Fluorochrome labeling

To analyze the changes in new cementum apposition rate, double fluorescence labeling was performed as described previously,[24] with a minor modification. Briefly, a calcein label[††] (12.5 mg/kg i.p.) was administered to mice 7 days after surgery. Alizarin red label[††] (30 mg/kg i.p.) was administered at 14 days after surgery. Mice were sacrificed at 30 days after surgery, and the mandibles were removed and fixed in 70% ethanol for 48 h. The specimens were dehydrated through a graded series of ethanol (70–100%) and embedded in methyl methacrylate[††] (MMA) without prior decalcification. Fifty-five micrometer-sections were cut using a saw microtome[‡‡] with tungsten carbide knife.[‡‡] The unstained sections were viewed under epifluorescent illumination using a microscope,[‖] interfaced with software[#] and camera.[¶]

Picrosirius red stain for collagen

In order to study the orientation and organization of the newly formed periodontal ligament tissue in the healing area, picrosirius red staining was used. Tissues processed for histology were stained with a picrosirius red staining kit according to manufacturer directions.[§§] Slides were immersed in 0.2% phosphomolybdic acid hydrate, rinsed in water, incubated in direct red 80 for 60 min, then 0.01 N HCl solution for an additional 2 min. Samples were rinsed in 75% ethanol for 45 sec, then dehydrated in xylene, cleared and mounted with coverslips. Digital images were captured with a light microscope[‖‖] fitted with a light polarizer, with a digital camera.[¶¶] Organization of PDL collagen fibers was visualized by turning polarizer to maximize signal in the PDL of all sections.

Immunohistochemistry

Immunohistochemistry (IHC) was performed as previously described.[20, 25] Mouse mandible tissues were deparaffinized in xylene and rehydrated using decreased graded dilutions of ethanol. Tissues were permeabilized in acetone at −20°C for 10 min, and endogenous peroxidase was quenched by incubation in 3% H_20_2 in methanol solution for 1 hr. Primary antibodies were used with biotinylated secondary antibodies[##] against rabbit or goat primary antibodies, as appropriate, and slides were developed using a 3-amino-9-ethylcarbazole (AEC) substrate kit.[##] Positive controls included staining in WT tissues, where immunolocalization of target proteins has been well characterized. Negative controls were performed lacking primary antibody. Primary antibodies used to react with mouse targets of interest included: rabbit anti-recombinant mouse bone sialoprotein (BSP), (a gift from Dr. Renny Franceschi, University of Michigan); rabbit anti-rat dentin matrix protein-1[***] (DMP1) raised against an N-terminal (90–111) portion of DMP1; goat anti-human NPP1;[†††] LF-175 rabbit anti-mouse osteopontin (OPN) (Dr. Larry Fisher, NIDCR).[26] IHC for each target protein was performed in sections from at least three WT and *Ank* KO

[††]Sigma-Aldrich, Saint Louis, MO, USA
[‡‡]Leica SM 2500, Leica Microsystems Nussloch GmbH, Nussloch, Germany.
[§§]Polysciences, Inc., Warrington, PA, USA
[‖‖]Nikon OptiPhot-2, Nikon Instruments Inc, Melville, NY, USA
[¶¶]Canon EOS 5D Mark II, Canon U.S.A., Inc., Lake Success, NY, USA
[##]Vector Laboratories, Inc., Burlingame, CA, USA.
[***] Takara Bio, Inc., Shiga, Japan
[†††] AbCam, Inc., Cambridge, MA, USA

animals for each age, with representative staining for selected antibodies shown in the Results section.

Statistical analysis

The null hypothesis of no difference between WT and KO groups regarding the evaluated parameters was tested by the parametric Student t-test and non-parametric Mann-Whitney test for linear and percent measurements, respectively with α=0.05.

RESULTS

Histological analysis of defect healing

The surgical wounds healed well with no signs of infection and no observable in growth of oral or skin epithelium into the defect. After surgeries, animals continued to feed normally and gain weight.

Histological sections from day 15 indicated newly formed bone and fibrous tissue scattered within the defect area in both *Ank* WT and KO mice (Figure 2A–D). The defect area could be identified by the reversal line, which clearly divided pre-existing and new-formed bone. New cementum, when observed, occurred adjacent to pre-existing cementum in the form of spicules or projections, being predominantly of cellular type and present more frequently in *Ank* KO mice.

By day 30, the overlying buccal alveolar bone was restored in both *Ank* WT and KO mice. In *Ank* KO at this time point, new cementum formation was present more consistently on cut root surfaces, compared to WT controls (Figure 2E–H). Neither root resorption nor ankylosis was observed in any of the groups at any time points.

Loss of ANK induced more rapid and increased cementum regeneration

Histomorphometry was employed to detect and quantify dimensions of cementum regeneration in *Ank* KO and WT, as well as determine if surrounding periodontal tissues were altered during defect repair. Defect filling was assessed at days 15 and 30 for unfilled space, soft tissue, and new bone, and no major differences were detected in % in *Ank* KO vs. WT controls (Figure 3A). Within the limits of analysis, no differences were observed in the proportion of mineralized (BD) in the new-formed bone in KO vs. WT mice (Figure 3B). Linear measurements for extension of new cementum (ENC) formation showed significantly greater extension of new cementum formation for the KO animals versus WT at 15 and 30 days after healing ($p<0.05$), approximately 4-fold at day 15 and 2-fold at day 30 (Figure 3C). Furthermore, the proportion of cementum-denuded root coverage by new cementum was significantly greater on the *Ank* KO cut root surface compared with WT, more than 2.5-fold at day 15 and more than 1.7-fold at day 30 (Figure 3D). Comparison of thickness of new cementum (TNC) in *Ank* KO vs. WT revealed that KO mice featured significantly greater deposition of new cementum along the cut root surface, a trend increasing with time (Figure 3E). Therefore, increased cementogenesis was detected by 15 days post-surgery, though the effect was even greater by day 30.

Progression of new cementum apposition was observed using vital fluorochrome labeling, with fluorescent microscopy performed on tissues harvested 30 days post-surgery. In regions of pre-existing cementum and bone outside of the defect area, calcein dye (green) injected at 7 days after surgery was observed with similar intensity in *Ank* KO and WT (Figure 4A–B). This dye, administered relatively early in the healing process, provided no evidence for cementum deposition in the defect region at 7 days post-surgery, for both WT and KO. The second fluorochrome, alizarin red (red) dye, injected at 14 days after surgery was observed

in both WT and *Ank* KO, suggesting some mineral deposition for both groups by this stage in healing. However, fluorochrome labeling lines in *Ank* KO cementum appeared consistently thicker and more concentrated than controls, indicating more rapid mineral deposition in the defect areas in *Ank* KO vs. controls.

Picrosirius red staining observed under polarized light enhances the natural birefringence of collagen, allowing assessment of collagen fiber organization.[27] At 30 days post-surgery in WT and KO, some PDL collagen fibers were observed to be parallel to the healing root surface. However, for both WT and KO, some organized and functionally oriented periodontal ligament fibers were also observed (Figure 4C–J).

Cementum regeneration in *Ank* KO recapitulates developmental changes in extracellular matrix proteins

To better understand the nature of the regenerated cementum and the mechanisms contributing to cementum regeneration in WT and *Ank* KO, immunohistochemistry (IHC) was used. We analyzed expression of selected cementum, bone, and dentin markers at days 15 and 30 during periodontal defect repair. Developmental expression of bone sialoprotein (BSP), osteopontin (OPN), dentin matrix protein 1 (DMP1), and ectonucleotide pyrophosphatase phosphodiesterase 1 (NPP1) was previously mapped during tooth root formation in *Ank* KO mice,[20] and expression during periodontal healing will be considered in the context of those findings.

BSP is present in bone and cementum extracellular matrix, and immunolocalizes as a concentrated band defining the acellular cementum layer. Staining of BSP in pre-existing bone was similar between WT and *Ank* KO. In WT, cementum was labeled by a positive, even staining, while BSP presence was more diffuse in KO. By 15 days post-surgery, BSP protein expression was clear in the new bone of WT and KO mice. Little BSP was immunolocalized to the healing root surface at this stage. By day 30, the thin layer of new cementum on WT roots featured a positive BSP staining reminiscent of the original AEFC layer. In KO, the regenerated cementum layer was BSP positive, though not uniformly so (Figures 5A–B and 5I–J for 15 and 30 days, respectively).

Osteopontin (OPN) is also present in bone and cementum, as well as in the soft tissue of the PDL. In the present investigation OPN was immunopositive in bone and cementum of both WT and KO. By day 15, OPN was localized to the healing root surfaces in both WT and *Ank* KO molars. Ank KO samples featured a larger, generally more intense zone of OPN-positive matrix and cells on the defect surface, as well as more intense OPN in the adjacent PDL. OPN staining was similar in WT vs. KO at 30 days, except for notably increased OPN in *Ank* KO PDL (Figures 5C–D and 5K–L for 15 and 30 days, respectively).

Dentin matrix protein 1 (DMP1) localized primarily to bone matrix around osteocytes, with lower levels of staining apparent in dentinal tubules. WT acellular cementum did not stain positively for DMP1. At day 15, there was no detectable DMP1 staining in healing sites either group. By day 30, DMP1 localized to the matrix and cells in *Ank* KO repair cementum, while in WT, DMP1 stained weakly and primarily around cementocytes (Figures 5E–F and 5M–N for 15 and 30 days, respectively).

We have identified low level expression of NPP1 in odontoblasts and osteoblasts, whereas cementoblasts associated with AEFC expressed higher levels of NPP1. [20] In the present study, by day 15, no NPP1 expression could be detected at the healing site in WT samples. In *Ank* KO at 15 days, NPP1 expression was strong in cementoblasts associated pre-existing cementum, but little expression was detected in the healing defect except in a small number of osteoblasts. By day 30, NPP1 expression in WT was detectable in some cementoblasts

and osteoblasts on regenerated tissues. Osteoblast NPP1 expression in *Ank* KO was similar to WT, though cementoblasts at the healing site exhibited increased NPP1 at this time point (Figures 5G–H and 5O–P for 15 and 30 days, respectively).

DISCUSSION

This is the first study to assess wound healing in mice using an isolated uniform periodontal wound healing model, while maintaining functional occlusion, without oral bacterial contamination or ingrowth of gingival epithelium into the wound space. This periodontal defect model, used previously by our group and others, has proven to be a predictable and reliable model for studying periodontal healing in rats.[22, 23, 28, 29] Although this model may not represent a critical-size defect for periodontal regeneration in mice, it serves as a reasonable screening model to examine wound-healing kinetics in the periodontium. Importantly, the experimental design also allowed us to ask the question whether a loss of gene function affecting cementum formation could be exploited to test the hypothesis that regeneration would recapitulate development.

In this study, periodontal regeneration in WT controls was compared with *Ank* KO mice, a model with reduced tissue PP_i that exhibits increased cementogenesis and hypercementosis.[20] Based on the developmental phenotype, we hypothesized that reduced extracellular PP_i levels would encourage greater cementum regeneration. As predicted, *Ank* KO mice featured significantly greater new-formed cementum vs. controls, at 15 and 30 days post-surgery ($p<0.05$). Further, vital fluorochrome labeling indicated more organized mineral deposition on the root surface in the defect areas in *Ank* KO vs. controls. At days 15 and 30 during healing, regenerating cementum and associated cells in *Ank* KO recapitulated expression patterns mapped during cementogenesis, including limited BSP and strong OPN and DMP1 in the cementum matrix, as well as elevated NPP1 in associated cementoblasts. Within the limits of the study, we found that reduced local levels of PP_i promoted increased cementum regeneration, suggesting that a novel strategy to reduce PP_i or modulate P_i/PP_i in the periodontal region may encourage greater and more predictable cementum regeneration.

Previous studies in mouse models and human patients have identified PP_i as an important regulator of the acellular cementum development, and this has provided the rationale for our current approach to cementum regeneration. Local cell and tissue level concentrations of PP_i are controlled primarily by a number of regulatory enzymes and transporters. Tissue nonspecific alkaline phosphatase (TNAP) is an ectoenzyme that hydrolyzes PP_i and is important for bone mineralization, as well as being active in the periodontal region.[13–15] The condition hypophosphatasia (HPP), which causes rickets, and osteomalacia, results from mutations in the gene for TNAP.[15, 30–32] HPP provided the first suggestion of the sensitivity of cementum to PP_i homeostasis because in both humans and mice, TNAP deficiency causes cementum aplasia or severe hypoplasia, poor periodontal attachment, and exfoliation of teeth.[15, 17, 19]

The progressive ankylosis protein (ANK) is a membrane spanning protein that regulates transport of intracellular PP_i to the extracellular space.[9–11] Another PP_i regulator, ectonucleotide pyrophosphatase phosphodiesterase 1 (NPP1), also increases extracellular PP_i, but by enzymatic hydrolysis of nucleoside triphosphates. ANK and NPP1 offset TNAP activity by increasing extracellular concentrations of the mineralization inhibitor, PP_i.[12] We have described the developmental tooth phenotype in mice lacking ANK or NPP1 function, characterized by a marked increase in cementum formation, while other tooth tissues (e.g. PDL, dentin, and alveolar bone) appeared unaffected.[16, 18, 20] While ANK, NPP1, and TNAP are widely expressed, we and others have identified increased expression and/or

activity in PDL vs. the pulp/dentin complex, highlighting the importance of PP_i metabolism in the Periodontia. [17, 20]

Here, we observed that loss of ANK function encouraged more robust cementum regeneration, resulting in significantly increased new cementum coverage of the root and thicker cementum in KO vs. control mice. In developmental studies, we found that PP_i governs appositional rate of the acellular cementum.[16, 20] We reasoned that in the context of the fenestration defect, putative progenitor cells would be available to repopulate the defect region and the lack of ANK function and the associated PP_i deficiency would create an environment conducive to cementogenesis. Histological observations, histomorphometry, and observation of more organized vital dye labeling in *Ank* KO tissues support our hypothesis. Some functionally oriented PDL fibers were identified on healing defect surfaces in KO as well as WT mice. Organization and insertion of PDL fibers in conjunction with rapid and predictable cementum formation provide an opportunity for true periodontal regeneration, i.e. a restoration of the structure and function of the periodontium.[1]

We analyzed expression of selected cementum, bone, and dentin markers during periodontal defect repair to better understand the nature of the regenerated cementum in WT and *Ank* KO, and to parallel mapping of these same factors in cementum development.[20] New cementum formation in WT defects was marked by positive labeling of BSP and OPN, classic markers for acellular cementum.[33–35] In defects in *Ank* KO mice, new cementum also mirrored developmental patterns, including limited BSP, strong OPN and DMP1 in the cementum matrix, and heightened NPP1 in associated cementoblast cells. We have demonstrated that these changes in AEFC composition in *Ank* KO teeth are the results of rapid and increased cementum apposition; as cementum thickness increases, BSP becomes limited, cementoblasts increase expression of OPN and NPP1 in response to increased apposition, and DMP1 is increased in the matrix around embedded cells (cementocytes).[20] We report here for the first time that loss of ANK caused altered cementoblast gene expression during defect healing, and importantly show that these changes recapitulate cementum development in this model.

CONCLUSIONS

These results serve as validation for a novel proof-of-principle concept for periodontal regeneration. Within the limits of the study, we found that reduced local levels of PP_i promoted increased cementum regeneration, suggesting that a novel strategy to reduce PP_i or modulate P_i/PP_i in the periodontal region may encourage greater and more predictable cementum regeneration. While more work must be done to better understand other mechanistic aspects of cementum regeneration, e.g. factors encouraging PDL fiber insertion in regenerating cementum in order to make a strong interface, the possibility for more rapid and predictable cementum formation is an encouraging step forward.

Acknowledgments

These studies were supported by São Paulo State Research Foundation (FAPESP, São Paulo, SP, Brazil) grant 08/00534-7 (FHNJ), NIH FIRCA (5R03TW007590-03) (MJS/FHNJ) and NIH/NIDCR grant DE15109 (MJS). The authors declare no conflicts of interest in these studies. The authors thank Jirawan Wade (University of Washington School of Dentistry) for preparation of plastic embedded sections. We thank Dr. Larry Fisher (NIH/NIDCR) and Dr. Renny Franceschi (University of Michigan School of Dentistry) for generously provided antibodies for these studies.

References

1. Bosshardt DD, Sculean A. Does periodontal tissue regeneration really work? Periodontol 2000. 2009; 51:208–219. [PubMed: 19878476]

2. Saygin NE, Giannobile WV, Somerman MJ. Molecular and cell biology of cementum. Periodontology 2000. 2000; 24:73–98. [PubMed: 11276875]

3. Bartold PM, McCulloch CA, Narayanan AS, Pitaru S. Tissue engineering: a new paradigm for periodontal regeneration based on molecular and cell biology. Perio 2000. 2000; 24:253–269.

4. Foster BL, Popowics TE, Fong HK, Somerman MJ. Advances in defining regulators of cementum development and periodontal regeneration. Curr Top Dev Biol. 2007; 78:47–126. [PubMed: 17338915]

5. Foster BL, Tompkins KA, Rutherford RB, et al. Phosphate: known and potential roles during development and regeneration of teeth and supporting structures. Birth Defects Res C Embryo Today. 2008; 84:281–314. [PubMed: 19067423]

6. Fleisch H, Bisaz S. Mechanism of calcification: inhibitory role of pyrophosphate. Nature. 1962; 195:911. [PubMed: 13893487]

7. Meyer JL. Can biological calcification occur in the presence of pyrophosphate? Arch Biochem Biophys. 1984; 231:1–8. [PubMed: 6326671]

8. Razzaque MS. The FGF23-Klotho axis: endocrine regulation of phosphate homeostasis. Nat Rev Endocrinol. 2009; 5:611–619. [PubMed: 19844248]

9. Ho AM, Johnson MD, Kingsley DM. Role of the mouse ank gene in control of tissue calcification and arthritis. Science. 2000; 289:265–270. [PubMed: 10894769]

10. Gurley KA, Reimer RJ, Kingsley DM. Biochemical and genetic analysis of ANK in arthritis and bone disease. American journal of human genetics. 2006; 79:1017–1029. [PubMed: 17186460]

11. Johnson K, Goding J, Van Etten D, et al. Linked deficiencies in extracellular PP(i) and osteopontin mediate pathologic calcification associated with defective PC-1 and ANK expression. J Bone Miner Res. 2003; 18:994–1004. [PubMed: 12817751]

12. Harmey D, Hessle L, Narisawa S, Johnson K, Terkeltaub R, Millán J. Concerted regulation of inorganic pyrophosphate and osteopontin by akp2, enpp1, and ank: an integrated model of the pathogenesis of mineralization disorders. Am J Pathol. 2004; 164:1199–1209. [PubMed: 15039209]

13. Groeneveld MC, Everts V, Beertsen W. Alkaline phosphatase activity in the periodontal ligament and gingiva of the rat molar: its relation to cementum formation. J Dent Res. 1995; 74:1374–1381. [PubMed: 7560388]

14. Groeneveld MC, Van den Bos T, Everts V, Beertsen W. Cell-bound and extracellular matrix-associated alkaline phosphatase activity in rat periodontal ligament. Experimental Oral Biology Group. Journal of periodontal research. 1996; 31:73–79. [PubMed: 8636879]

15. Whyte MP. Hypophosphatasia and the role of alkaline phosphatase in skeletal mineralization. Endocr Rev. 1994; 15:439–461. [PubMed: 7988481]

16. Nociti FH Jr, Berry JE, Foster BL, et al. Cementum: a phosphate-sensitive tissue. J Dent Res. 2002; 81:817–821. [PubMed: 12454094]

17. van den Bos T, Handoko G, Niehof A, et al. Cementum and dentin in hypophosphatasia. J Dent Res. 2005; 84:1021–1025. [PubMed: 16246934]

18. Fong H, Foster BL, Sarikaya M, Somerman MJ. Structure and mechanical properties of Ank/Ank mutant mouse dental tissues--an animal model for studying periodontal regeneration. Arch Oral Biol. 2009; 54:570–576. [PubMed: 19338977]

19. Beertsen W, VandenBos T, Everts V. Root development in mice lacking functional tissue non-specific alkaline phosphatase gene: inhibition of acellular cementum formation. J Dent Res. 1999; 78:1221–1229. [PubMed: 10371245]

20. Foster BL, Nagatomo KJ, Bamashmous SO, et al. The Progressive Ankylosis Protein Regulates Cementum Apposition and Extracellular Matrix Composition. Cells Tissues Organs. 2011

21. Gurley KA, Chen H, Guenther C, et al. Mineral Formation in Joints Caused by Complete or Joint-Specific Loss of ANK Function. J Bone Miner Res. 2006; 21:1238–1247. [PubMed: 16869722]

22. King GN, King N, Cruchley AT, Wozney JM, Hughes FJ. Recombinant human bone morphogenetic protein-2 promotes wound healing in rat periodontal fenestration defects. J Dent Res. 1997; 76:1460–1470. [PubMed: 9240382]

23. Benatti BB, Neto JB, Casati MZ, Sallum EA, Sallum AW, Nociti FH Jr. Periodontal healing may be affected by aging: a histologic study in rats. Journal of periodontal research. 2006; 41:329–333. [PubMed: 16827728]
24. Lu Y, Ye L, Yu S, et al. Rescue of odontogenesis in Dmp1-deficient mice by targeted re-expression ofDMP1 reveals roles for DMP1 in early odontogenesis and dentin apposition in vivo. Dev Biol. 2007; 303:191–201. [PubMed: 17196192]
25. Chu E, Fong H, Blethen F, et al. Ablation of systemic phosphate-regulating gene fibroblast growth factor 23 (Fgf23) compromises the dentoalveolar complex. Anat Rec (Hoboken). 2010; 293:1214–1226. [PubMed: 20583265]
26. Ogbureke KU, Fisher LW. Expression of SIBLINGs and their partner MMPs in salivary glands. J Dent Res. 2004; 83:664–670. [PubMed: 15329369]
27. Junqueira L, Bignolas G, Brentani R. Picrosirius staining plus polarization microscopy, a specific method for collagen detection in tissue sections. Histochem J. 1979; 11:447–455. [PubMed: 91593]
28. Zhao M, Jin Q, Berry JE, Nociti FH Jr, Giannobile WV, Somerman MJ. Cementoblast delivery for periodontal tissue engineering. J Periodontol. 2004; 75:154–161. [PubMed: 15025227]
29. Huang K, Shen C, Chiang C, Hsieh Y, Fu E. Effects of bone morphogenetic protein-6 on periodontal wound healing in a fenestration defect of rats. J Periodontal Res. 2005; 40:1–10. [PubMed: 15613073]
30. Whyte, MP. Hypophosphatasia Nature's window to alkaline phosphatase in man. In: Bilezikian, JP.; Raisz, LG.; Rodan, GA., editors. Principles of Bone Biology. Vol. I. San Diego, CA: Academic Press; 2002. p. 1229-1248.
31. Millan, JL. Mammalian Alkaline Phosphatases. Weinheim: Wiley-VCH Verlag GmbH & Co. KGaA; 2006. p. 322
32. Narisawa S, Frohlander N, Millan JL. Inactivation of two mouse alkaline phosphatase genes and establishment of a model of infantile hypophosphatasia. Dev Dyn. 1997; 208:432–446. [PubMed: 9056646]
33. MacNeil R, Berry J, D'Errico J, Strayhorn C, Piotrowski B, Somerman M. Role of two mineral-associated adhesion molecules, osteopontin and bone sialoprotein, during cementogenesis. Connect Tissue Res. 1995; 33:1–7. [PubMed: 7554941]
34. McKee M, Zalzal S, Nanci A. Extracellular matrix in tooth cementum and mantle dentin: localization of osteopontin and other noncollagenous proteins, plasma proteins, and glycoconjugates by electron microscopy. Anat Rec. 1996; 245:293–312. [PubMed: 8769669]
35. Bronckers A, Farach-Carson M, Van Waveren E, Butler W. Immunolocalization of osteopontin, osteocalcin, and dentin sialoprotein during dental root formation and early cementogenesis in the rat. J Bone Miner Res. 1994; 9:833–841. [PubMed: 8079659]

Summary

In a mouse periodontal fenestration model, *Ank* KO and reduced local levels of PP_i promoted increased cementum regeneration, more rapid and organized apposition, and recapitulation of developmental gene expression and matrix composition.

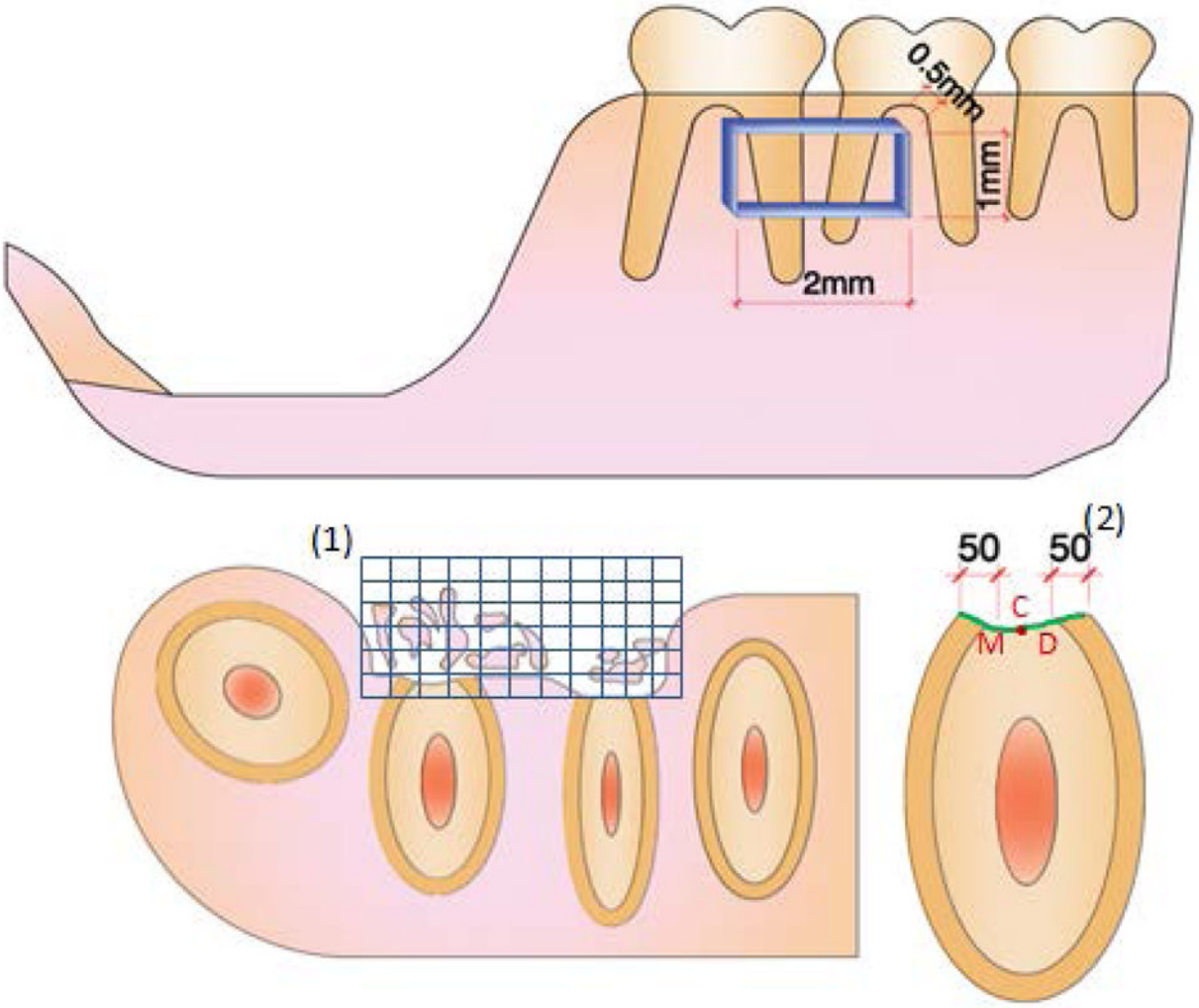

Figure 1. Schematic illustration of the assessed histomorphometric parameters

Histomorphometry was used to assess percentage of defect filling (DF) (%), proportion of mineralized tissue (BD) (%), extension of new cementum (ENC) (μm), proportion of cementum-denuded root coverage by new cementum (PRC) (%) and thickness of new cementum (TNC) (μm). DF and BD were measured using a square grid (1) overlaid on the defect area. ENC was obtained by linear measurement of newly formed cementum, and PRC determined by the proportion of newly formed cementum covering the total extent of the instrumented root (green line). TNC measurements were made at fixed distances of 50 μm from mesial (M) and distal (D) side of pre-existing cementum, and on the central (C) region of the instrumented root (2).

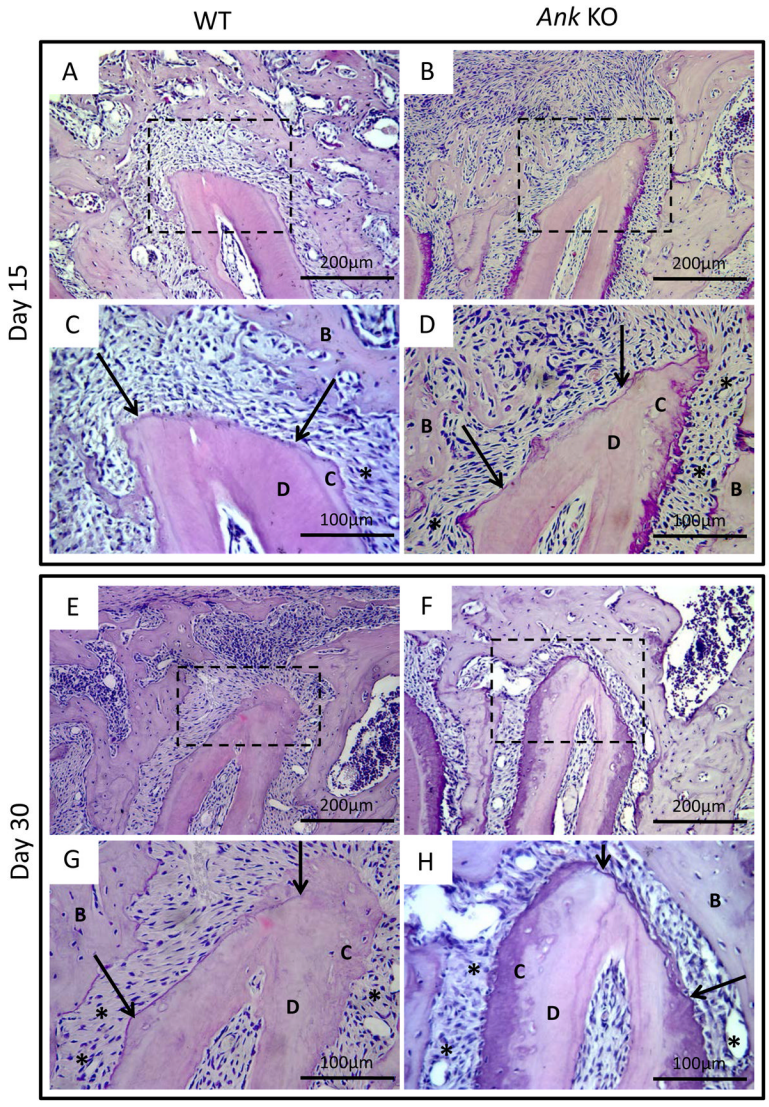

Figure 2. Histological analysis of periodontal defect healing in WT and *Ank* KO

Representative H&E stained slides from WT and Ank KO mice at 15, and 30 days post-surgery. Arrows indicate margins of pre-existing cementum and rectangles define the instrumented root area used for linear measurements that is also presented in higher magnification. At 15 days post-surgery, both WT and *Ank* KO roots featured newly formed bone and fibrous tissue. New cementum, predominantly of the cellular type, was observed more frequently in *Ank* KO mice. By day 30, restoration of overlying alveolar bone was observed in defects in both WT and *Ank* KO mice. In *Ank* KO at this time point, new cementum formation was present more consistently on all cut root surfaces, compared to WT controls - Original magnification: figures A, B, E and F: 200x and figures C, D, G and H: 400x. *Abbreviations: B: bone; D: dentin, C: cementum, star: periodontal ligament.*

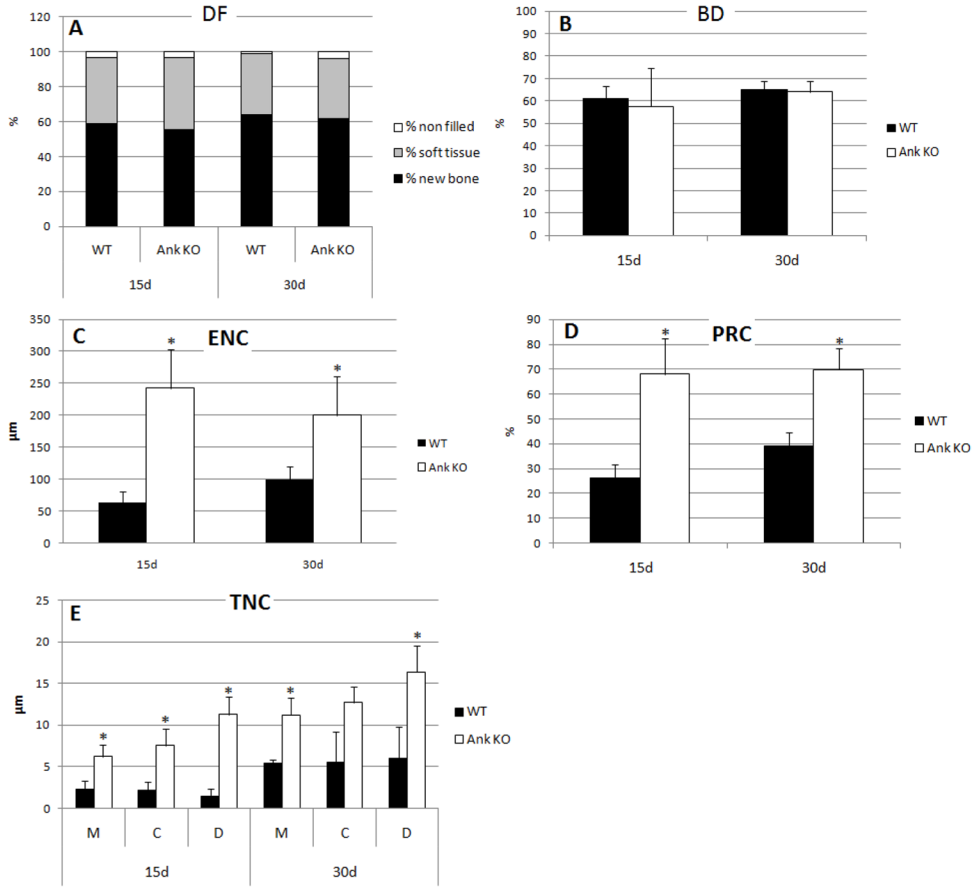

Figure 3. Histomorphometry confirmed loss of ANK induced more rapid and increased cementum regeneration

Histomorphometric approaches are described in the Methods and Figure 1. **(A)** No major differences were detected in defect filling parameters in *Ank* KO vs. WT at days 15 and 30. **(B)** New bone density (BD) was not different in *Ank* KO vs. WT at both time points. **(C)** Extension of new cementum (ENC) and **(D)** the proportion of root coverage by new cementum (PRC) were significantly increased in *Ank* KO vs. WT at 15 and 30 days. **(E)** Thickness of new cementum (TNC) measured at mesial side of the root (M), center of the root (C), and distal side of the root (D) was greater for all parameters in *Ank* KO vs. WT. * $p<0.05$.

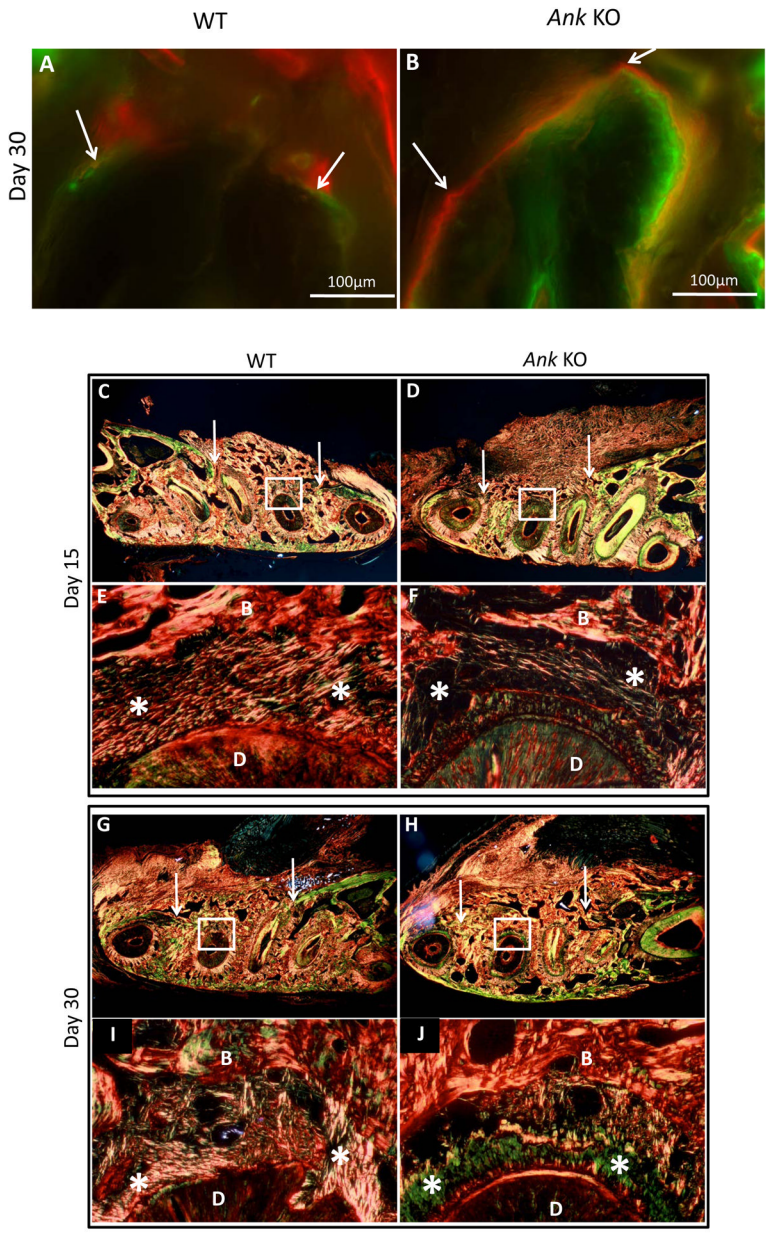

Figure 4. Labeling of new cementum apposition and periodontal ligament fiber organization

(A–B) In regions of pre-existing cementum and bone away from the defect area, calcein dye (green) injected 7 days after surgery was observed with similar intensity in WT and *Ank* KO. Alizarin labeling (red) injected at day 14 was observed in WT and KO, though staining in *Ank* KO appear thicker and more concentrated than in controls. **(C–J)** Low magnification photographs of the surgically-created periodontal defects in the mandibles. Arrows indicate margins of defect and rectangles define the instrumented root area that is presented in higher magnification. Note that at 15 days post-surgery, both groups featured new bone formation (woven-like bone) with a disorganized connective tissue interfaced between the tooth and the new bone. At day 30, bone was more mature-like with regions of organized, parallel and functionally oriented PDL fibers identified in both WT and KO - Original magnification: figures C, D, G and H: 200x and figures E, F, I and J: 400x. *Abbreviations: B: bone; D: dentin, star: periodontal ligament.*

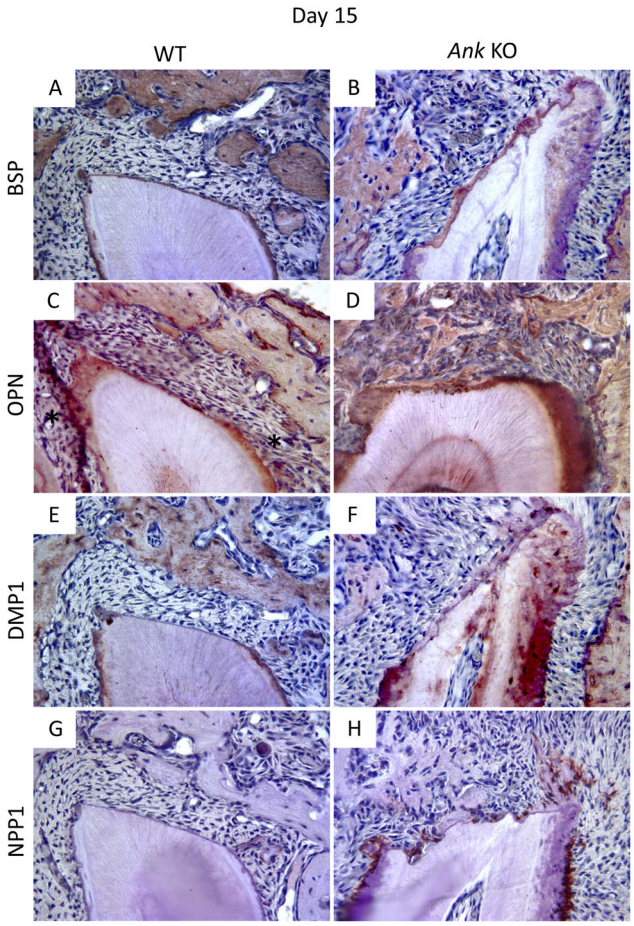

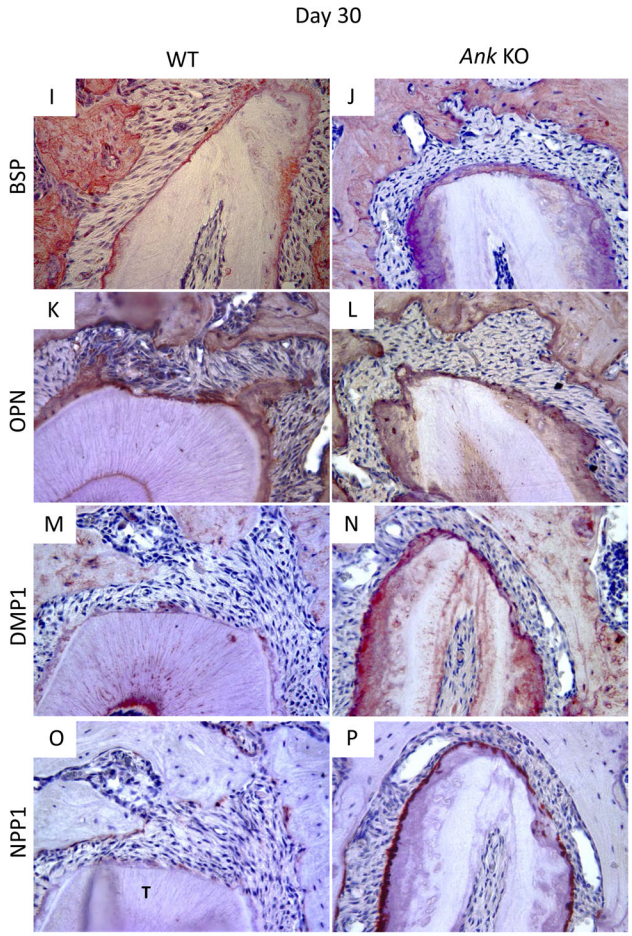

Figure 5. Expression of mineralized tissue markers during cementum regeneration

Histological sections from days 15 and 30 were used for IHC. **(A–B/I–J) Bone sialoprotein (BSP):** By day 15, BSP protein expression was clear in the new bone of WT and KO mice, though little BSP was localized to the healing root surface. By day 30, the thin layer of new cementum on WT and KO roots featured positive BSP staining. **(C–D/K–L) Osteopontin (OPN):** OPN was positive in bone and cementum of WT and KO. By day 15, OPN was localized to the healing root surfaces in both WT and *Ank* KO molars, though more intense OPN staining was consistently identified in KO new cementum and PDL. OPN staining was similar in WT vs. KO at 30 days, except for notably increased OPN in *Ank* KO PDL. **(E–F/M–N) Dentin matrix protein 1 (DMP1):** DMP1 localized primarily to bone matrix around osteocytes, with lower levels of staining apparent in dentinal tubules. WT acellular cementum did not stain positively for DMP1. At day 15, there was no detectable DMP1 staining in healing sites either group. By day 30, DMP1 localized strongly to matrix and cells in *Ank* KO repair cementum, while in WT, DMP1 stained weakly and primarily around cementocytes. **(G–H/O–P) Ectonucleotide pyrophosphatase phosphodiesterase 1 (NPP1):** By day 15, no NPP1 expression could be detected at the healing site in WT samples, though in *Ank* KO, NPP1 expression was strong in cementoblasts associated pre-existing cementum. By day 30, NPP1 was detectable in some WT cementoblasts and osteoblasts on regenerated tissues. Osteoblast NPP1 expression in *Ank* KO was similar to WT, though cementoblasts at the healing site exhibited increased NPP1 -Original magnification: 400x.